Proceedings of the 2006 IEEE International Conference on Robotics and Automation
Orlando, Florida - May 2006

A Hierarchical Control Strategy for the Autonomous Navigation of a Ducted Fan Flying Robot

Jean Michel Pflimlin
LAAS-CNRS
Toulouse, FRANCE
Email: pflimlin@laas.fr

Tarek Hamel
I3S - UNSA - CNRS
Sophia Antipolis, FRANCE
Email: thamel@i3s.unice.fr

Philippe Soueres
LAAS-CNRS
Toulouse, FRANCE
Email: soueres@laas.fr

Robert Mahony
Department of Engineering,
Australian National University
ACT, 0200, AUSTRALIA
Email: mahony@ieee.org

***Abstract*— This paper describes a control strategy to stabilize the position of a Vertical Takeoff and Landing (VTOL) Unmanned Aerial Vehicle (UAV) in wind gusts. The proposed approach takes advantage of the cascade structure of the system to design a hierarchical controller. The idea is to separate the controller in a High Level Controller devoted to position control and a Low Level Controller devoted to stabilization and attitude control. Both controllers are designed by means of backstepping techniques that allow the stabilization of the vehicle's position while on-line estimation of the unknown aerodynamic forces. The global stability of the connected system is proven, and simulations as well as experimental results are presented.**

I. Introduction

The design of autonomous navigation strategies for ducted fan Micro Aerial Vehicles (MAV) has now become a very challenging research area [1], [2], [3]. These small and discreet secure platforms, able to perform vertical takeoff and landing (VTOL) and stationary flight, are of evident interest for civil and military operations in an urban environment. The Bertin Technology company is currently working on the development of such a ducted fan UAV, called HoverEye. A view of the HoverEye is given Fig. 1. The work presented in this paper has been developed in the framework of a collaboration between Bertin Technologies and the laboratories LAAS-CNRS and I3S. The objective of this collaboration is to model the system and develop autonomous control strategies. It must be able to perform hovering flight for surveillance applications despite possible wind perturbations. The automatic control design must allow the vehicle to be easily operated by an inexperienced user. At the end, the vehicle is expected to execute autonomous flights, defined by sequences of navigation points, while avoiding encountered obstacles.

In this paper, we take advantage of the pyramidal structure of the system to design a hierarchical controller made of a high level position control and a low level attitude control. This architecture of controller is usual in most of schemes of Guidance, Navigation and Control algorithms. The difficulty, when designing control laws for connected systems, is to ensure the stability of the global system. In linear applications, the proof is immediate, because of exponential stability of each subsystem. This property is lost in nonlinear applications.

In [4], the authors proposed a hierarchical controller to realize path following with a helicopter in hover mode, and achieved global convergence of the system. However, in their application, the aerodynamic efforts were neglected, thus both translational and rotational dynamics were exponentially stable. Here, the estimation of unknown aerodynamic efforts leads to an asymptotic stability of the rotational dynamics, whereas the translational dynamics is exponentially stable. The main contribution of this paper is to show that it is still possible to ensure the asymptotic stability of the global system.

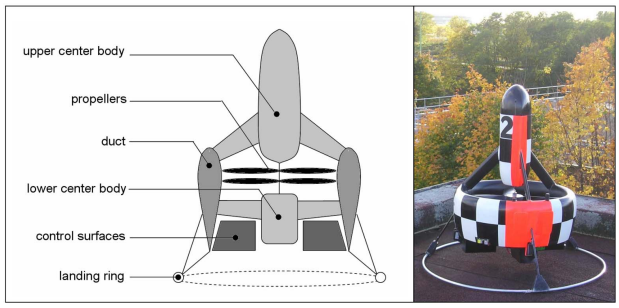

1: A view of the ducted fan VTOL UAV HoverEye

The paper is articulated as follows: section II is devoted to the description of the vehicle dynamics with a focus on the cascade structure of the system. The control design is described in section III and a proof of stability of the proposed strategy is given. Simulation results and experiments are described in section IV to illustrate the concept. The last section contains concluding remarks.

II. Modelling

In this section, we briefly present the kinematic parameters and the dynamic representation associated to the system. Any further detail may be found in [5]. We would like to focus in this section on the representation of the system as two connected subsystems.

A. Kinematics

Two reference frames are considered (see [6]):

- $\mathcal{I}$ is the inertial frame attached to the earth. It is assumed to be Galilean. It is associated to the vector basis $\{\mathbf{x_0}, \mathbf{y_0}, \mathbf{z_0}\}$: $\mathbf{x_0}$ points to the North, $\mathbf{y_0}$ to the East, and $\mathbf{z_0}$ to the center of Earth. (see Fig. 2)
- $\mathcal{A}$ is the body-fixed frame attached to the vehicle. It is associated to the vector basis $\{\mathbf{x_b}, \mathbf{y_b}, \mathbf{z_b}\}$: the roll axis

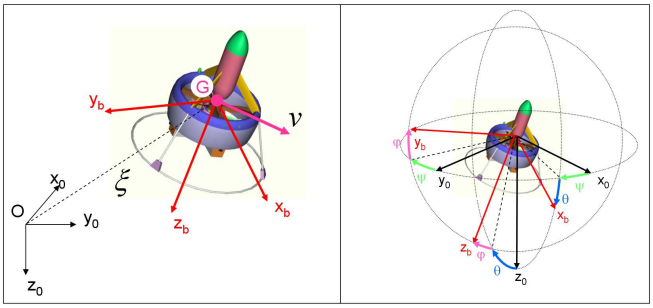

2: Inertial and body fixed frames - Aeronautical Euler angles parameterization of attitude

$\mathbf{x_b}$ points forwards, the pitch axis $\mathbf{y_b}$ points to the right and the yaw axis $\mathbf{z_b}$ points downwards.

The kinematic parameters used to describe the movement of this 6 DoF rigid body are $[\xi, v, R, \Omega]$:

- ξ is the position of the center of gravity with respect to $\mathcal{I}$, expressed in the inertial frame: $\xi = \left[\overrightarrow{OG}\right]_{\mathcal{I}}$
- v is the velocity of the center of gravity with respect to $\mathcal{I}$ expressed in the inertial frame: $v = \left[\overrightarrow{V}(G/\mathcal{I})\right]_{\mathcal{I}}$
- $R = [\mathbf{x_b}, \mathbf{y_b}, \mathbf{z_b}]_{\mathcal{I}}$ is the transformation matrix from $\mathcal{I}$ to $\mathcal{A}$, usually parameterized by the aeronautical Euler angles (ϕ, θ, ψ), as shown in Fig. 2
- $\Omega = [p, q, r]^T$ is the angular velocity vector of $\mathcal{A}$ relative to $\mathcal{I}$, expressed in the body fixed frame: $\Omega = \left[\overrightarrow{\Omega}_{(\mathcal{A}/\mathcal{I})}\right]_{\mathcal{A}}$

B. Dynamic Representation

The different forces acting on the system are described in [5]. The resulting representation of the dynamics is[1][2]:

$$\begin{bmatrix} \dot{\xi} \\ m\dot{v} \\ \dot{R} \\ \mathbf{J}\dot{\Omega} \end{bmatrix} = \begin{bmatrix} v \\ -uRe_3 + mge_3 + F_{ail} + F_{ext} \\ R\text{sk}(\Omega) \\ -\text{sk}(\Omega)\mathbf{J}\Omega + \Gamma_{ail} + \varepsilon\text{sk}(e_3)R^T F_{ext} \end{bmatrix} \quad (1)$$

In the model (1), m and $\mathbf{J} = diag(J_1, J_1, J_2)$, with $J_1 > J_2$, denote respectively the mass and the inertia matrix of HoverEye. The thrust u and the moment $\Gamma_{ail} = [\Gamma_l, \Gamma_m, \Gamma_n]^T$ created by the control surfaces are the control inputs of the system. The external aerodynamic efforts, F_{ext}, and the lever arm ε, are unknown parameters. As the point of application of F_{ext} is supposed to be on the yaw axis, ε is a scalar. An estimation of these parameters will be obtained via the proposed control strategy. The control surfaces also create the so-called small body forces F_{ail}, making the system strictly non minimum phase. One of the main contribution in [5] was to show that by considering the following variable change:

$$\begin{cases} \xi_D = \xi + dRe_3 \\ v_D = v + dR\Omega_\times e_3 \\ \bar{u} = u + md(p^2 + q^2) \end{cases} \quad \text{with} \quad d = -\frac{J_1}{mL}$$

[1] $\text{sk}(\Omega)$ denotes the skew symmetric matrix associated to Ω: $\forall u, v \in \mathbb{R}^3$, $\text{sk}(u)v = u \times v = -v \times u = -\text{sk}(v)u$

[2] $\{e_1, e_2, e_3\}$ denotes the canonical base of $\mathbb{R}^3$: $e_1 = [1, 0, 0]^T$, $e_2 = [0, 1, 0]^T$, $e_3 = [0, 0, 1]^T$

It was possible to use in control design the equivalent model:

$$\begin{bmatrix} \dot{\xi}_D \\ m\dot{v}_D \\ \dot{R} \\ \mathbf{J}\dot{\Omega} \end{bmatrix} = \begin{bmatrix} v_D \\ -\bar{u}Re_3 + mge_3 + F_{ext} \\ R\text{sk}(\Omega) \\ \Gamma_{ail} + \varepsilon\text{sk}(e_3)R^T F_{ext} \end{bmatrix} \quad (2)$$

as long as the yaw rate r is maintained to zero. Therefore, one of the main objective in the control strategy will be to regulate r to zero. We will see in section III-B that the structure of the controller naturally implies this regulation.

C. Cascade Structure of the System

We rewrite the system as two connected subsystems. The first one describes the translational dynamics: the magnitude $\bar{u}$ and the direction $n = Re_3$ of the thrust represent its control inputs. The second subsystem describes the dynamics of the direction of the thrust n along with the vector Γ_{ail} is the control input. The equivalent inter-connection scheme appears in the block 'HoverEye Dynamics' in Fig. 3.

Lemma 1: Let $n = Re_3$ be the unit direction of the thrust, $\omega = R\Omega$ the components of the angular velocity in the inertial frame, $\gamma_{ail} = R\mathbf{J}^{-1}\Gamma_{ail}$ and $m_{ext} = (\varepsilon/J_1)F_{ext}$. The model (2) is equivalent to:

$$(\Sigma_1) \quad : \quad \begin{bmatrix} \dot{\xi}_D \\ m\dot{v}_D \end{bmatrix} = \begin{bmatrix} v_D \\ -\bar{u}n + mge_3 + F_{ext} \end{bmatrix} \quad (3)$$

$$(\Sigma_2) \quad : \quad \begin{bmatrix} \dot{n} \\ \dot{\omega} \end{bmatrix} = \begin{bmatrix} \omega \times n \\ \gamma_{ail} + n \times m_{ext} \end{bmatrix} \quad (4)$$

Proof. The time derivative of n is given by[3]:

$$\dot{n} = \dot{R}e_3 = R\text{sk}(\Omega)e_3 = \text{sk}(R\Omega)Re_3$$

Introducing $\omega = R\Omega$, one has finally: $\dot{n} = \text{sk}(\omega)n$. The time derivative of ω is given by:

$$\dot{\omega} = \dot{R}\Omega + R\dot{\Omega} = \underbrace{R\,\text{sk}(\Omega)\Omega}_{=0} + R\mathbf{J}^{-1}\Gamma_{ail} + R\mathbf{J}^{-1}\varepsilon\text{sk}(e_3)R^T F_{ext}$$

One will notice that $\mathbf{J}^{-1}\text{sk}(e_3) = (1/J_1)\text{sk}(e_3)$. It yields:

$$\dot{\omega} = \gamma_{ail} + R\text{sk}(e_3)R^T m_{ext} = \gamma_{ail} + \text{sk}(Re_3)m_{ext}$$

□

III. Control Design

In this section, we design a controller in two parts: the High Level Controller is dedicated to position control in which the magnitude $\bar{u}$ and the direction n of the thrust are considered as control inputs. The Low-Level controller is designed to stabilize the attitude n of the vehicle to the n_d required by the High Level Controller. Figure 3 represents the resulting block diagram in closed loop. The global stability of the system with both controllers in cascade is proven in section III-C.

[3] keep in mind a basic property of skew symmetric matrices: $\forall u \in \mathbb{R}^3, \forall R \in SO(3), R\text{sk}(u)R^T = \text{sk}(Ru)$

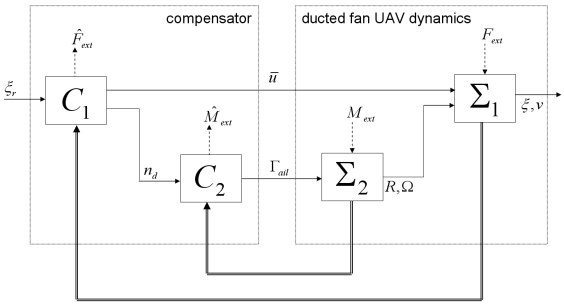

3: Block diagram of the architecture of the controller

A. Position Control Design

Let ξ_s be a constant desired position for the control point D. In this section, a control law is designed to ensure hovering flight at point ξ_s despite quasi constant wind. Aerodynamic forces are supposed to be unknown, but constant (their fluctuations are slow compared to the vehicle dynamics: $\dot{F}_{ext} = 0$). The controller will provide an estimation $\hat{F}_{ext}$ of F_{ext}. The control law must define magnitude and orientation of the thrust in order to counteract perturbing wind forces.

Lemma 2: Let $\{\lambda_1, \lambda_2, \lambda_3\} \in \mathbb{R}_+^*$. *Define* $\{a, b, c\} \in \mathbb{R}_+^*$ *as:*

$$a = \textstyle\sum_i \lambda_i, \quad b = \sum_{i<j} \lambda_i \lambda_j, \quad c = \prod_i \lambda_i$$

We assume that the discriminant $\Delta = b^2 - 4ac$ *is positive. Define the gains* k_1, k_2, k_F *as:*

$$k_2 = a, \quad k_1 = \tfrac{b - \sqrt{\Delta}}{2a}, \quad k_F = \tfrac{b + \sqrt{\Delta}}{2} \tag{5}$$

And the following error terms:

$$\begin{array}{lll} \delta_1 & = \xi_D - \xi_s & \textit{Position error} \\ \delta_2 & = mk_1\delta_1 + mv_D & \textit{Velocity error} \\ \tilde{F}_{ext} & = F_{ext} - \hat{F}_{ext} & \textit{Estimation error} \end{array} \tag{6}$$

The system (3) is exponentially stabilizable with the control law on the thrust vector:

$$\bar{u}n_d = k_2\delta_2 + \hat{F}_{ext} + mge_3 \tag{7}$$

and the following adaptive filter on F_{ext}*:*

$$\dot{\hat{F}}_{ext} = k_F\delta_2 \tag{8}$$

Moreover, the adaptive filter converges to the real value of F_{ext}*. More precisely,* $\xi \longrightarrow \xi_s$ *and* $\hat{F}_{ext} \longrightarrow F_{ext}$*.*

Proof. Let us define $x = [\delta_1, \delta_2, \tilde{F}_{ext}]^T$. The idea of the proof is to write $\dot{x} = Ax$ with the matrix A Hurwitz. First, when differentiating δ_1, it yields, using (6) and (2):

$$\dot{\delta}_1 = \dot{\xi}_D = v_D = -k_1\delta_1 + \frac{\delta_2}{m}$$

The first term in the expression of $\dot{\delta}_1$ corresponds to a desired velocity that would mean an exponential convergence of δ_1 to zero. δ_2 represents the gap between this virtual control and the actual velocity v_D of the vehicle. Differentiating δ_2, it comes, using (6) and (2):

$$\begin{array}{rcl} \dot{\delta}_2 & = & mk_1\dot{\delta}_1 + m\dot{v}_D \\ & = & -mk_1^2\delta_1 + k_1\delta_2 - \bar{u}n + mge_3 + F_{ext} \end{array}$$

In the expression of $\dot{\delta}_2$, the unknown term F_{ext} and the control input vector $\bar{u}n$ are written as follows:

$$\begin{array}{rl} F_{ext} & = \hat{F}_{ext} + \tilde{F}_{ext} \\ \bar{u}n & = \bar{u}n_d + \bar{u}(n - n_d) \end{array}$$

Using the definition of $\bar{u}n_d$ given by (7), the following expression of $\dot{\delta}_2$ is obtained:

$$\dot{\delta}_2 = -mk_1^2\delta_1 + (k_1 - k_2)\delta_2 + \tilde{F}_{ext} + \bar{u}(n_d - n)$$

Finally, differentiating the term $\tilde{F}_{ext}$, using (8), it yields:

$$\dot{\tilde{F}}_{ext} = \dot{F}_{ext} - \dot{\hat{F}}_{ext} = -k_F\delta_2$$

As far as the translational dynamics are concerned, we assume that $n_d \equiv n$. The following linear state space representation of the translational dynamics is then obtained:

$$\underbrace{\begin{bmatrix} \dot{\delta}_1 \\ \dot{\delta}_2 \\ \dot{\tilde{F}}_{ext} \end{bmatrix}}_{\dot{x}} = \underbrace{\begin{bmatrix} -k_1 & \frac{1}{m} & 0 \\ -mk_1^2 & k_1 - k_2 & 1 \\ 0 & -k_F & 0 \end{bmatrix}}_{A} \underbrace{\begin{bmatrix} \delta_1 \\ \delta_2 \\ \tilde{F}_{ext} \end{bmatrix}}_{x}$$

Now, let us verify that the set of gains $\{k_1, k_2, k_F\}$ ensures that A is Hurwitz:

$$\begin{array}{rl} \det(\lambda I - A) = & (\lambda + k_1)(\lambda(\lambda - k_1 + k_2) + k_F) + \frac{1}{m}mk_1^2\lambda \\ = & \lambda^3 + k_2\lambda^2 + (k_1k_2 + k_F)\lambda + k_1k_F \end{array}$$

Using (5) and proceeding by identification, it yields:

$$\begin{array}{rl} \det(\lambda I - A) & = \lambda^3 + a\lambda^2 + b\lambda + c \\ & = (\lambda + \lambda_1)(\lambda + \lambda_2)(\lambda + \lambda_3) \end{array}$$

And therefore the matrix A is Hurwitz. It yields that δ_1 and $\tilde{F}_{ext}$ converge exponentially to zero. □

Note that n is not really a control input so we cannot impose $n = n_d$. We design in next section an attitude control to ensure asymptotic convergence of the error term $\tilde{n} = n_d - n$ and then we ensure the global stability of the connected systems.

B. Attitude Control Design

In this section, we suppose in the control design that the desired thrust n_d is constant, that is to say $\dot{n}_d = 0$. This hypothesis is acceptable because the rotational dynamics is tuned up to be much faster than the translational dynamics. Rigorously, the expression of n_d given by the controller C_1 should be derived and added to the command on Γ_{ail}. This approach was taken in [5]. The hypothesis made here simplifies the resulting control law.

Lemma 3: Let n_d *be a constant desired orientation of the thrust. Let* k_n*,* k_ω*,* k_m *be positive constants. Define the following error terms:*

$$\begin{array}{lll} \delta & = \omega - k_n(n \times n_d) & \textit{Angular error} \\ \tilde{m}_{ext} & = m_{ext} - \hat{m}_{ext} & \textit{Estimation error} \end{array}$$

The system (4) is asymptotically stabilizable with the control law on the moment created at G *by the control surfaces:*

$$\gamma_{ail} = -k_\omega\delta - n \times n_d + k_n(\omega \times n) \times n_d - n \times \hat{m}_{ext} \tag{9}$$

and the estimation filter on $\hat{m}_{ext}$:

$$\dot{\hat{m}}_{ext} = k_m(\delta \times n) \tag{10}$$

Moreover, the yaw rate is maintained to zero. More precisely, $n \to n_d$ and $r \to 0$.

Proof. Proof is achieved by mean of backstepping procedure:
Step 1. Consider the following candidate function:

$$S_1 = 1 - n_d^T n$$

n and n_d being two unit vectors, one may verify that for any n, S_1 is positive and vanishes iff $n = n_d$. Using (4) and the basic property of triple scalar product[4], we get:

$$\dot{S}_1 = -n_d^T \dot{n} = -n_d^T(\omega \times n) = -\omega^T(n \times n_d)$$

If the angular velocity was a control input of system (Σ_2), the command $\omega_c = k_1(n \times n_d)$, with $k_1 > 0$, would ensure the non positivity of $\dot{S}_1$:

$$\dot{S}_1 = -k_n|n \times n_d|^2$$

and therefore the convergence of n to n_d[5]. However, as ω is not a control input, we define the gap $\delta = \omega - k_n(n \times n_d)$. At the end of the first step of Backstepping, one has:

$$\begin{array}{rl} \dot{S}_1 = & -k_n|n \times n_d|^2 + \delta^T(n \times n_d) \\ \delta = & \omega - k_n(n \times n_d) \end{array} \tag{11}$$

Step 2. In order to ensure the convergence to zero of δ, we add this gap in a candidate Lyapunov function S_2. In the expression of $\dot{\delta}$, the unknown aerodynamic moment m_{ext} will appear. In order to counteract this perturbation, we introduce an estimation $\hat{m}_{ext}$ of m_{ext}. The estimation error $\tilde{m}_{ext}$ is included in the expression of S_2:

$$S_2 = S_1 + \frac{1}{2}|\delta|^2 + \frac{1}{2k_m}|\tilde{m}_{ext}|^2$$

The time derivative of S_2 is given by:

$$\dot{S}_2 = \dot{S}_1 + \delta^T\dot{\delta} + \frac{1}{k_m}\tilde{m}_{ext}^T\dot{\tilde{m}}_{ext}$$

m_{ext} is supposed to be constant, thus $\dot{\tilde{m}}_{ext} = -\dot{\hat{m}}_{ext}$. Moreover using (11) and (4), it comes:

$$\dot{\delta} = \dot{\omega} - k_n(\dot{n} \times n_d) = \gamma_{ail} + n \times m_{ext} - k_n(\omega \times n) \times n_d$$

At this stage, using the control law (9) and the expression of $\dot{S}_1$ given by (11), $\dot{S}_2$ expresses as:

$$\dot{S}_2 = -k_n|n \times n_d|^2 - k_\omega|\delta|^2 + \delta^T(n \times \tilde{m}_{ext}) - \frac{1}{k_m}\tilde{m}_{ext}^T\dot{\hat{m}}_{ext}$$

Once again, using the properties of the triple scalar product, one has $\delta^T(n \times \tilde{m}_{ext}) = \tilde{m}_{ext}^T(\delta \times n)$. Therefore, the adaptive filter defined in (10) ensures the non positivity of the Lyapunov function time derivative $\dot{S}_2$:

$$\dot{S}_2 = -k_n|n \times n_d|^2 - k_\omega|\delta|^2$$

This expression of $\dot{S}_2$ guarantees the convergence of $n \times n_d$ and of δ to zero. The component of δ along the yaw axis being $n^T\delta = n^T\omega = e_3^T\Omega = r$, the convergence of δ to zero maintains r to zero, as required to cancel the term $\Omega \times \mathbf{J}\Omega$. □

C. Stability of the Connected Systems

In this section, we demonstrate the asymptotic stability of the connected systems. When connecting both controllers, a perturbing term $\tilde{n} = n_d - n$ appears in the translational dynamics. The controller (C_2) makes this term converge to zero. The system (Σ_1), stabilized by the control (7), may express as:

$$\dot{x} = Ax + B\bar{u}\tilde{n} \quad \text{with} \quad \tilde{n} \to 0$$

Where $x = [\delta_1, \delta_2, \tilde{F}_{ext}]^T$ and $B = [0,1,0]^T$. Let $K = [0, k_2, -1]$, then $\bar{u}$ is:

$$\bar{u} = |Kx + mge_3 + F_{ext}|$$

Theorem 1: The feedback control on $\bar{u}$ (7) and the control law (9) on the control surfaces makes the system (2) asymptotically stable. The adaptive filters (8) and (10) provide an estimation of the aerodynamic forces F_{ext} and the lever arm ε. More precisely, introducing:

$$\hat{\varepsilon} = J_1\frac{(n \times \hat{F}_{ext})^T(n \times \hat{m}_{ext})}{|n \times \hat{F}_{ext}|^2}$$

One has: $\xi_D \to \xi_d$, $\hat{F}_{ext} \to F_{ext}$ and $\hat{\varepsilon} \to \varepsilon$.

Proof. The proof is achieved in three steps:

- First, we show that the system cannot escape in finite time, which means that $x(t)$ is defined $\forall t > 0$.
- Then, we show that there exists a time t_2 such that $\forall t \geq t_2$, the time derivative of the Lyapunov function is negative, ensuring the convergence of the connected systems.
- Finally, the theorem of Lasalle allows to demonstrate the convergence of the different terms.

The proof is inspired by the more general results on cascade systems proposed in [7]. The matrix A is Hurwitz, yielding:

$$\exists P, Q > 0 \quad \text{s.t.} \quad A^TP + PA = -Q$$

Let us consider the following candidate Lyapunov V:

$$V(x) = x^TPx \quad \Rightarrow \quad \dot{V} = -x^TQx + 2x^TPB\bar{u}\tilde{n}$$

Let us deal with the perturbing term $2x^TPB\bar{u}\tilde{n}$. Let p_2 be the second column of the matrix P. It yields:

$$PB = p_2$$

In the expression of $\bar{u}$, we put apart the term linear with respect to x from the rest of the perturbing term. It yields:

$$\bar{u} \leq |Kx| + |mge_3 + F_{ext}|$$

[4]Recall that, $\forall a, b, c \in \mathbb{R}^3$, the triple scalar product is defined as:

$$a^T(b \times c) = b^T(c \times a) = c^T(a \times b) = \det([a, b, c])$$

[5]If we denote by α the angle (n, n_d), then one has $S_1 = 1 - \cos\alpha$. The virtual control ω_c leads to $\dot{S}_1 = -k_n(\sin\alpha)^2$, which ensures $\alpha \to 0$, and therefore $n \to n_d$.

Introducing:

$$\Delta = p_2|mge_3 + F_{ext}|\tilde{n}$$

It comes:

$$2x^T PB\bar{u}\tilde{n} \leq 2|p_2|.|K|.|\tilde{n}|.|x|^2 + 2x^T\Delta$$

Introducing the matrix:

$$Q_1 = Q - 2|p_2|.|K|.|\tilde{n}|I_n \tag{12}$$

the time derivative of V can be bounded from above as follows:

$$\dot{V} \leq -x^T Q_1 x + 2x^T\Delta \tag{13}$$

At this stage, we cannot ensure that the matrix Q_1 is definite positive. However, it is clear, in the expression (12), that for $\tilde{n}$ small enough, the matrix Q will become preponderant, leading to positive definiteness of the matrix Q_1. As $\tilde{n}$ tends to zero, it exists a time for which the matrix Q_1 will become positive definite. However, we have to ensure first that the state of the system is well defined $\forall t \geq 0$, that is to say a finite time escape cannot occur.

Step 1. Denoting by $\lambda_{min}(P)$ the smallest eigenvalue of matrix P, and introducing $\alpha, \beta > 0$ defined by:

$$\alpha = \frac{||Q_1||}{\lambda_{min}(P)} \quad \text{and} \quad \beta = \frac{2|\Delta|}{\sqrt{\lambda_{min}(P)}}$$

it yields:

$$\dot{V} \leq \alpha V(x) + \beta\sqrt{V(x)}$$

Now, proceed by contradiction to prove that a finite time escape cannot occur. Let us suppose there exists a time t_{max} such that $t \to t_{max}$ means $V(t) \to +\infty$. Then we can build a sequence $(t_k)_{k\geq 1}$ that tends to t_{max} It yields:

$$\forall t \in [t_1, t_k], \quad \tfrac{dV}{dt} \leq \alpha V + \beta\sqrt{V}$$

Therefore, when integrating along the interval $[t_1, t_k]$, one has:

$$\int_{V(t_1)}^{V(t_k)} \frac{dV}{\alpha V + \beta\sqrt{V}} \leq \int_{t_1}^{t_k} dt$$

When k tends to infinity, it yields:

$$\int_{V(t_1)}^{+\infty} \frac{dV}{\alpha V + \beta\sqrt{V}} \leq (t_{max} - t_1)$$

However, as the integral in the left member is infinite over the interval $[V(t_1), +\infty[$ while the right term is finite, this leads to a contradiction. Therefore, the system may not diverge in finite time and $x(t)$ is defined $\forall t > 0$.

Step 2. As $||\tilde{n}|| \to 0$, $\exists t_2$ such that:

$$\forall t \geq t_2, \quad ||\tilde{n}|| < \frac{\lambda_{min}(Q)}{2||p_2||.||K||}$$

Using the definition of Q_1 given by (12), it yields $\forall t \geq t_2$, the matrix Q_1 is definite positive. Therefore, it can be written using the Cholesky decomposition:

$$Q_1 = U^T U$$

I: parameters of the vehicle

Name	Value	Unit
g	9.80	ms^{-2}
m	3.0	kg
I_1	0.1	kgm^2
I_2	0.03	kgm^2
L	0.2	m
ε	-0.05	m

Where U is an upper triangular matrix. Using the above decomposition, the inequality (13) is equivalent to:

$$\dot{V} \leq -|Ux - U^{-T}\Delta|^2 + \Delta^T Q_1^{-1}\Delta$$

Such a bounding ensures that the system converges to a compact domain around the point $x_e = Q_1^{-1}\Delta$ of radius $||U^{-T}\Delta||$. As Δ tends to zero, this domain tends asymptotically to the equilibrium point $x = 0$.

Step 3. The theorem of Lasalle implies $\xi \to \xi_s$ and $\hat{F}_{ext} \to F_{ext}$. The direction of the thrust converges to a constant direction n^∞ verifying: $|F_{ext} + mge_3)|n^\infty = F_{ext} + mge_3$. The convergence of system (4) yields $(\delta, \dot{\delta}) \to 0$. Using (9), $\dot{\delta}$ expresses as:

$$\dot{\delta} = -k_\omega\delta - n \times n_d + n \times \tilde{m}_{ext}$$

Therefore, one has $n \times \tilde{m}_{ext} \to 0$, meaning $n \times \hat{m}_{ext} \to n^\infty \times m_{ext}$. Taking $t \to +\infty$ in the expression of $\hat{\varepsilon}$ yields:

$$\hat{\varepsilon} \to J_1 \frac{(n^\infty \times \hat{F}_{ext})^T (n^\infty \times m_{ext})}{|n^\infty \times \hat{F}_{ext}|^2}$$

As $\hat{F}_{ext} \to F_{ext}$ and $m_{ext} = (\varepsilon/J_1)F_{ext}$, it yields $\hat{\varepsilon} \to \varepsilon$. □

IV. Simulations and Experiments

A. Simulations

In this section, we present simulation results to illustrate the efficiency of the method. First, a simulation was performed on the ideal model (2) used for control design, in order to illustrate the convergence properties shown in Theorem 1. We chose in Table I parameters representative of this kind of vehicle. The controller has been run with the following gains:

$$k_1 = 0.25 \quad k_2 = 2.1 \quad k_f = 0.51$$
$$k_n = 4 \quad k_\omega = 8 \quad k_m = 6$$

The vehicle, initially at position $\xi(0) = [0; 0; -5]$ is required to reach final position $\xi_s = [1; 2; -4]$, while a constant wind generates an effort $F_{ext} = [8N, 4N, 0]^T$. Results are presented in Figure 4. The vehicle reaches the desired position while the parameters F_{ext} and ε are correctly estimated.

In another simulation, we tested the robustness of the proposed controller on a simulator highly representative of the behavior of the vehicle, which includes a dynamic model of the actuators, an error model of imperfect sensors, and a model of the aerodynamical efforts determined by wind tunnel tests. The vehicle is required to reach the same position. At $t = 10s$, a step of wind reaching 4m/s is simulated along $\mathbf{x_0}$. Figure 5 shows the response of the vehicle, as

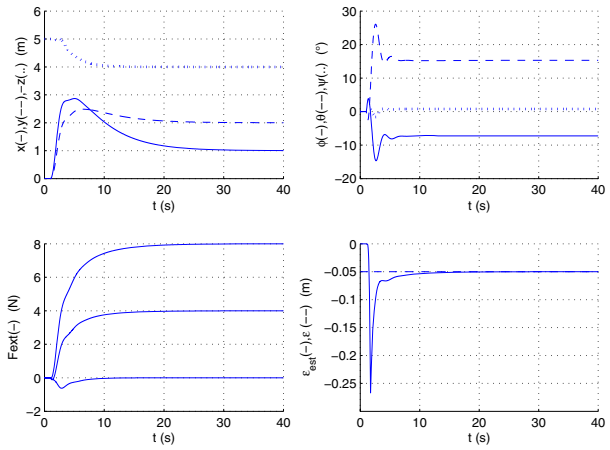

4: hovering flight in constant wind on the model (2)

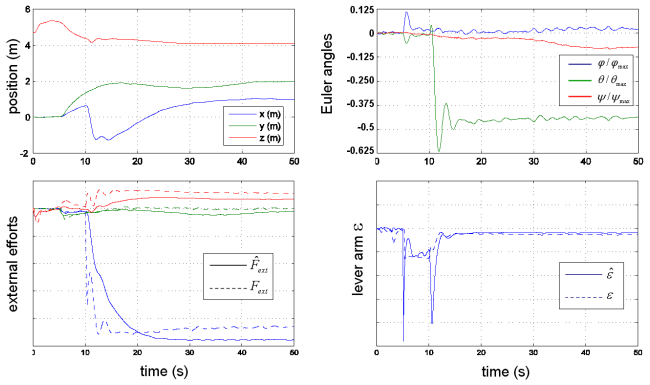

5: hovering flight in constant wind

well as the estimation of the unknown parameters. Adaptive control is usually sensitive to sensor noise and unmodelled dynamics. However, even though the estimated parameters only converge to a neighborhood of the real ones due to unmodelled dynamics, the vehicle stabilizes its position to the desired one.

B. Flight tests

The hierarchical controller has been implemented on the vehicle to demonstrate the autonomous waypoint navigation capability. To perform usual proportional navigation, we modify the definition of δ_2 in the position control:

$$\delta_2 = m(\mathrm{sat}_{V_c}(k_1\delta_1) + v_D), \quad \mathrm{sat}_a(x) = a\tanh\left(\frac{|x|}{a}\right)\frac{x}{|x|}$$

where V_c is the desired cruise speed between two waypoints. When the vehicle is near enough to the current waypoint, it takes as desired point ξ_s the next waypoint programmed by the operator on the ground control station. Figure 6 shows the resulting trajectory in the horizontal plane.

V. Conclusion

We have proposed a decoupled strategy to perform position control of a ducted fan UAV operating in constant wind. The method takes advantage of the connected structure of the system to design a controller dedicated to position control and another one dedicated to attitude stabilization. Global stability of the connected system has been proved, even though only asymptotic stability can be achieved on the rotational dynamics. Both controllers structure can be easily implemented in real time. Flight tests have been performed to demonstrate the waypoint navigation capability. In further work, the authors plan to reuse this framework to on-line local obstacle avoidance algorithms.

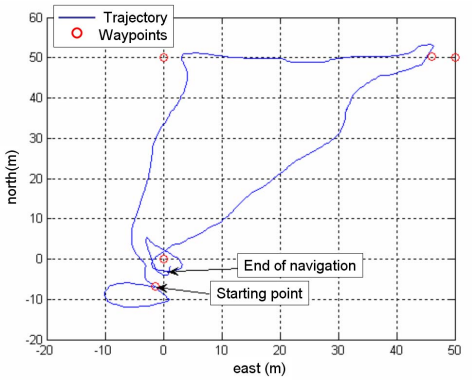

6: Flight test demonstrating the waypoint navigation capability

Acknowledgments

The authors wish to express their gratitude to the French Ministry of Research and Technology and the National Direction of Armament DGA for granting this research program. They also thank Olivier Philippe, VTOL UAV project manager at Bertin Technologies, who provided funding and support in this research. They also address a special thanks to the whole drone team of Bertin Technologies for their assistance.

References

[1] T. Hamel, R. Mahony, R. Lozano, and J. Ostrowski, "Dynamic modelling and configuration stabilization for an x4-flyer," in *Proceedings of the 15th International Federation of Automatic Control World Congress*. Barcelona, Spain: IFAC, October 2002, pp. 200–212.

[2] J. Fleming, T. Jones, P. Gelhausen, and D. Enns, "Improving control system effectiveness for ducted fan vtol uavs operating in crosswinds," in *Proceedings of the 2nd "Unmanned Unlimited" System, Technologies and Operations-Aerospace*, no. 2003–6514. San Diego, USA: AIAA, September 2003.

[3] I. Guerrero, K. Londenberg, P. Gelhausen, and A. Myklebust, "A powered lift aerodynamic analysis for the design of ducted fan uavs," in *Proceedings of the 2nd "Unmanned Unlimited" System, Technologies and Operations-Aerospace*, no. 2003–6557. San Diego, USA: AIAA, September 2003.

[4] K. Pathak and S. Agrawal, "An integrated spatial path planning and controller design approach for a hover-mode helicopter model," in *Proceedings of the 20th International Conference on Robotics and Automation*. Barcelona, Spain: IEEE, Avril 2005.

[5] J.-M. Pflimlin, P. Souères, and T. Hamel, "Hovering flight stabilization in wind gusts for a ducted fan uav," in *Proc. of the 43rd IEEE Conference on Decision and Control, CDC04*, Atlantis, Bahamas, December 2004.

[6] J. Boiffier, *The Dynamics Of Flight*. Jhon Wiley & Sons, 1998.

[7] E. Panteley and A. Loria, "Growth rate conditions for stability of cascaded time-varying systems," *Automatica*, vol. 37, no. 3, pp. 453–460, 2001.